ISSN 1674-1056
http://cpb.iphy.ac.cn
http://iopscience.iop.org/cpb
中国物理 B
Chinese Physics
中国物理
Chinese Physics B

Optical design of common-aperture multispectral and polarization optical imaging system with wide field of view

Xin Liu(刘鑫), Jun Chang(常军), Shuai Feng(冯帅), Yu Mu(穆郁), Xia Wang(王霞), Zhao-Peng Xu(徐兆鹏)

Citation: Chin. Phys. B . 2019, 28(8): 084201. **doi:** 10.1088/1674-1056/28/8/084201
Journal homepage: http://cpb.iphy.ac.cn; http://iopscience.iop.org/cpb

What follows is a list of articles you may be interested in

Investigation and optimization of sampling characteristics of light field camera for flame temperature measurement

Yudong Liu(刘煜东), Md. Moinul Hossain, Jun Sun(孙俊), Biao Zhang(张彪), Chuanlong Xu(许传龙)
Chin. Phys. B . 2019, 28(3): 034207. **doi:** 10.1088/1674-1056/28/3/034207

Anti-detection technology of cat eye target based on decentered field lens

Da-Lin Song(宋大林), Jun Chang(常军), Yi-Fei Zhao(赵一菲), Ze-Xia Zhang(张泽霞)
Chin. Phys. B . 2018, 27(9): 094220. **doi:** 10.1088/1674-1056/27/9/094220

Aberration correction of conformal dome based on rotated cylindrical lenses for ultra-wide field of regard

Linyao Yu(虞林瑶), Yongfeng Hong(洪永丰), Zhifeng Cheng(程志峰), Bao Zhang(张保)
Chin. Phys. B . 2018, 27(1): 014202. **doi:** 10.1088/1674-1056/27/1/014202

Application of optical diffraction method in designing phase plates

Ze-Min Lei(雷泽民), Xiao-Yan Sun(孙晓艳), Feng-Nian Lv(吕凤年), Zhen Zhang(张臻), Xing-Qiang Lu(卢兴强)
Chin. Phys. B . 2016, 25(11): 114201. **doi:** 10.1088/1674-1056/25/11/114201

General design basis for a final optics assembly to decrease filamentary damage

Sun Xiao-Yan, Lu Xing-Qiang, Lü Feng-Nian, Zhang Guo-Wen, Zhang Zhen, Yin Xian-Hua, Fan Dian-Yuan
Chin. Phys. B . 2015, 24(5): 054209. **doi:** 10.1088/1674-1056/24/5/054209

Optical design of common-aperture multispectral and polarization optical imaging system with wide field of view*

Xin Liu(刘鑫)[1], Jun Chang(常军)[1,†], Shuai Feng(冯帅)[1], Yu Mu(穆郁)[1,2], Xia Wang(王霞)[1], and Zhao-Peng Xu(徐兆鹏)[3]

[1] *School of Optics and Photonics, Beijing Institute of Technology, Beijing* 100081, *China*
[2] *Tianjin Jinhang Institute of Technical Physics, Tianjin* 300192, *China*
[3] *China Centre for Resources Satellite Data and Application, Beijing* 100191, *China*

(Received 21 February 2019; revised manuscript received 3 May 2019; published online 9 July 2019)

Multispectral and polarization cameras that can simultaneously acquire the spatial, spectral, and polarization characteristics of an object have considerable potential applications in target detection, biomedical imaging, and remote sensing. In this work, we develop a common-aperture optical system that can capture multispectral and polarization information. An off-axis three-mirror optical system is mounted on the front end of the proposed system and used as a common-aperture telescope in the visible light (400 nm–750 nm) and long-wave infrared (LWIR, 8 μm–12 μm) waveband. The system can maintain a wide field of view (4.5°) and it can demonstrate an enhanced identification ability. The off-axis three-mirror system gets rid of central obscuration while further yielding stable system resolution and energy. Light that has passed through the front-end common-aperture reflection system is divided into the visible light and LWIR waveband by a beamsplitter. The two wavebands then converge on two detectors through two groups of lenses. Our simulation results indicate that the proposed system can obtain clear images in each waveband to meet the diverse imaging requirements.

Keywords: optical design, common-aperture, multispectral imaging, polarization imaging

PACS: 42.15.–I, 42.15.Dp, 42.15.Fr, 42.79.–e **DOI:** 10.1088/1674-1056/28/8/084201

1. Introduction

Spectral imaging detects two-dimensional (2D) spatial information about multiple wavelengths with two spatial coordinates and one spectral dimension.[1–7] Polarization imaging acquires the information about target's features, shapes, texture, and material composition.[8–10] Multispectral and polarization imaging[11,12] can obtain the polarization information of an object in different wavelengths and thus becomes an effective detection technique[13–15] to improve target detection, biomedical imaging, remote sensing, and disease diagnosis. Image multiplexing methods produce multiple images by taking advantages of lens arrays,[16] beamsplitters,[17] image slicers,[18] Wollaston prisms,[19] light pipes[20,21] or active optical elements.[22] The simultaneous acquisition of multispectral and polarization images is a critical factor of the performance of multispectral and polarimetric imaging system. However, the majority of current multispectral imaging devices still feature the major limitation of measuring polarization and spectral information simultaneously. The simultaneous acquisition of polarization and spectral information leads to the dramatical increase of either system complexity[23] or time consumption.[24] For example, a multispectral single-shot polarimeter[25] can obtain only the polarization information of a linear pixel array. Therefore, scanning has to be included to enable the simultaneous acquisition of the multispectral and polarization information of a two-dimensional (2D) scene.

In this work, we design a relatively simple system for achieving the simultaneous acquisition of multispectral and polarization optical images. The system utilizes a catadioptric optical system to acquire polarization information in two diverse wavebands simultaneously. An off-axis reflection optical system is employed as a common-aperture telescope[26,27] to maintain a wide field of view (FOV), compared with some of the literature like Ref. [27] whose FOV is 1°. The optical system enhances the identification ability of the whole system by functioning in the full waveband. The off-axis three-mirror system gets rid of central obscuration by decenter and/or tilt[28] and stabilizes overall system resolution and energy. A beamsplitter separates light into the visible (400 nm–750 nm) and long-wave infrared (LWIR, 8 μm–12 μm) waveband. Visible light and LWIR light converge on two detectors once they pass through two sets of transmissive lenses. The simulation results indicate that the performance of the proposed system is quite satisfactory to obtain clear images in the visible spectrum and LWIR.

2. System design

As schematically illustrated in Fig. 1, the multispectral and polarization camera system can simultaneously acquire the spatial and polarization characteristics of an object in two

*Project supported by the National Natural Science Foundation of china (Grant No. 61471039).
†Corresponding author. E-mail: optics_chang@126.com
© 2019 Chinese Physical Society and IOP Publishing Ltd

different wavebands. The whole system functions in the visible light (400 nm–750 nm) and LWIR (8 μm–12 μm) wavebands and employs a catadioptric optical system. Two wavebands share a non-confocal optical system as a telescope. The optical system is mounted on the front of the camera system and overcomes the disadvantages encountered in the broad spectrum by the anti-reflection (AR) film coatings of refractive optical system. The non-confocal optical system can maintain a wide FOV (4.5°) and enhances the identification ability of the overall system by utilizing an off-axis three-mirror optical system as a common-aperture telescope. A beamsplitter is used to separate the emergent light path into the visible light and LWIR wavebands. These two different wavebands are employed in a refractive optical system for secondary imaging. The refractive optical system use a secondary telescope, a polarizer, and an objective to focus the visible light and LWIR wavebands on the detector. The common-aperture multispectral and polarization optical imaging system is thus realized.

The target is imaged multiple times to limit the size of the beamsplitter and polarizer aperture.

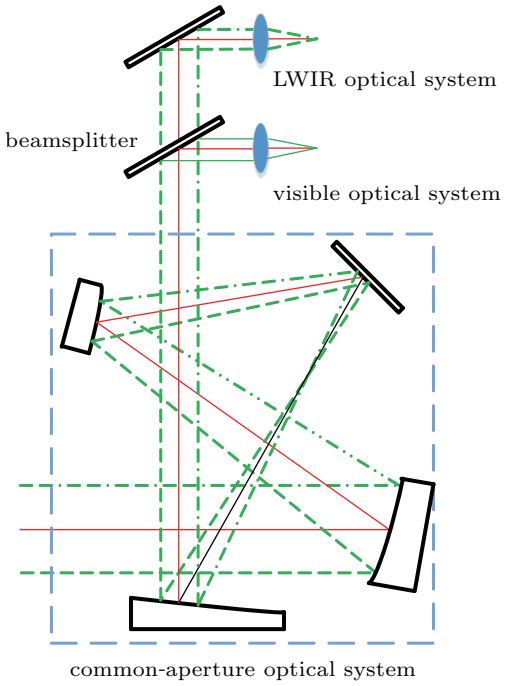


Fig. 1. Schematic diagram of common-aperture multispectral and polarization optical imaging system.

2.1. Common-aperture off-axis reflection optical system

Options for materials with the desired thermal properties, resilience, and color correction ability for a multispectral system are limited. Simultaneous optical imaging in the visible light and LWIR is necessary to increase the level of target discrimination and identification and reduce the rate of false alarm. We present a non-confocal common-aperture optical system in which an off-axis reflection system is used to achieve these objectives. Reflection systems have been attracting considerable attention from researchers because they do not exhibit chromatic aberration while possessing compact and light-weight structures. The off-axis three-mirror optical system has sufficient tunable parameters to reduce aberrations while getting rid of central obscuration and influences on resolution and energy. In addition to these advantages, there are other two reasons for employing this common-aperture off-axis reflection optical system: our front-end off-axis reflection optical system can not only achieve common-aperture in visible spectrum and LWIR, but also compress the beam to the ratio of 3.

The designed off-axis three-mirror common-aperture optical system is shown in Fig. 1. This system can maintain a wide FOV (4.5°) and meanwhile enhance the identification ability of the overall system. The focus of the combined first and second mirror is the same as that of the third mirror. Thus, a primary imaging plane is present between plane mirror and third mirror. The optical length L of the non-confocal optical system is given by the following formula:

$$L = F_{1,2} + \mathrm{F}_3 \tag{1}$$

where $F_{1,2}$ is the focal length of the combination of the first and second mirror, and F_3 is the focal length of the third mirror. A plane mirror that is inclined 45° is used to reduce the volume of the off-axis reflection system. The diameter of the exit beam is assumed to be limited to the diameter of the beamsplitter ($\varphi \leq 50$ mm) and polarizer ($\varphi \leq 40$ mm). The magnification of the non-confocal optical system must be reduced to increase angular magnification within a finite range and to limit the diameter of the exit beam. We select the magnification of the non-confocal optical system MR as 1:3 in consideration of the FOV; that is,

$$M_{\mathrm{R}} = -\frac{\mathrm{F}_3}{F_{1,2}} = \frac{D_{\mathrm{EXP}}}{D_{\mathrm{ENP}}}, \tag{2}$$

where D_{EXP} is the diameter of the exit pupil, and D_{ENP} is the diameter of the entrance pupil.

2.2. LWIR optical system

2.2.1. Secondary telescope

We should further limit the diameter of the exit beam, given the small size of the polarizer ($\varphi \leq 40$ mm). As shown in Fig. 2, we add a secondary telescope, such as a Kepler telescope, to limit the aperture diameter of the exit beam. We then limit the axial and lateral sizes of the objectives sequentially. An intermediate image exists between the first and second lens group.

The optical length L_{IR} of the secondary telescope is given by

$$L_{IR} = f_{IR1} + f_{IR2}, \tag{3}$$

where f_{IR1} and f_{IR2} are the focal length of the first lens group and that of the second lens group, respectively. The magnification of secondary telescope M_{IR} is selected as 2:3, that is,

$$M_{IR} = -\frac{f_{IR2}}{f_{IR1}} = \frac{d_{IR2}}{d_{IR1}}. \tag{4}$$

The FOV of the incident beam of secondary telescope changes from 4.5° to 13.5° after the incident beam has passed through the off-axis reflection optical system with a magnification of 1:3.

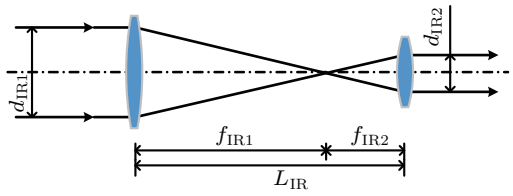


Fig. 2. Schematic diagram of Kepler telescope.

2.2.2. Objective

The objective converges beams on the detector and corrects residual aberration. These functions are illustrated schematically in Fig. 3.

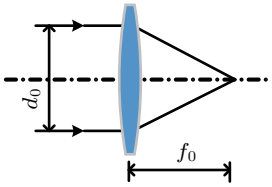


Fig. 3. Schematic diagram of objective.

The diameter of objective d_0 is given as

$$d_0 = D_{ENP} * M_R * M_{IR}. \tag{5}$$

2.3. Visible-spectrum optical system

The principle of the visible-spectrum optical system is similar to that of the LW system, which includes a secondary telescope and objective. These two systems can be distinguished as follows: A Kepler telescope is employed in the LW system, whereas a Galileo telescope is used in the visible-spectrum optical system. These differences are presented in Fig. 4. The optical length L_{LW} of the secondary telescope is given by

$$L_V = f_{V1} + f_{V2}, \tag{6}$$

where f_{V1} and f_{V2} are the focal length of the first lens group and that of the second lens group, respectively. Here the magnification of the secondary telescope M_V is chosen as 2:3, that is,

$$M_V = -\frac{f_{V2}}{f_{V1}} = \frac{d_{V2}}{d_{V1}}. \tag{7}$$

Like the LW system, the visible-spectrum optical system has an FOV of 4.5°.

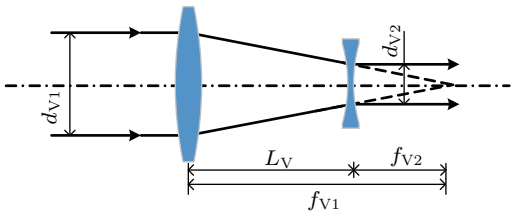


Fig. 4. Schematic diagram of Galileo telescope.

2.4. Polarizer

The polarizer, which is placed between the secondary telescope and the objective, is a key component of the multispectral and polarization optical imaging system. We can obtain the polarization information of images with different polarization states that can be modulated by rotating the polarizer in discrete steps. The diameters and incident angles of the polarizers are supposed to be controlled because polarizer diameters are generally less than 40 mm and accepted angle values are often within ±20°.

3. Simulation and results

We allocate the power of system elements and calculate the initial structural parameters in accordance with primary aberration theory and the design theory presented in Section 2.

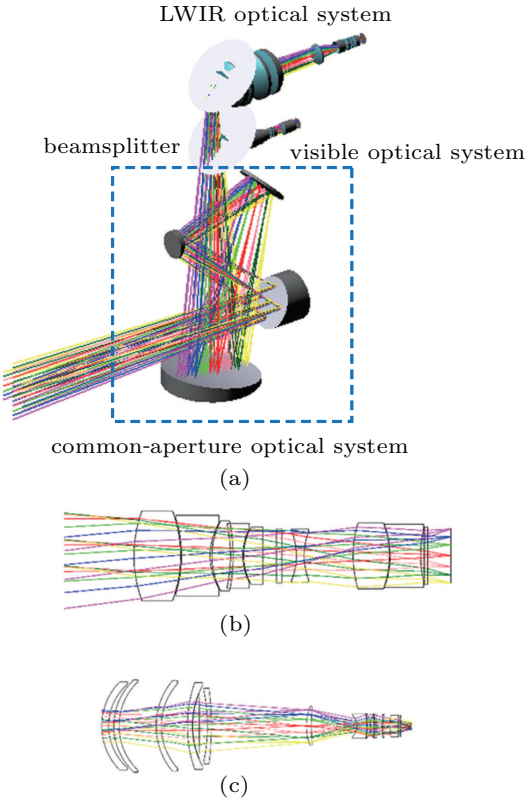


Fig. 5. Optical layout of the common-aperture multispectral and polarization optical imaging system. (a) Optical path of whole system. (b) Optical path of LWIR optical system. (c) Optical path of visible-spectrum optical system.

At first, the paraxial lens is used to meet first order requirements and then replaced by a real lens. After the elimination of aberration and a series of optimization, the common-aperture multispectral and polarization optical imaging system with an FOV of 4.5° is achieved. The system enables the aberration correction and the balance between primary aberration and advanced aberration. The diagram in Fig. 5 illustrates the design results. The whole system employs a catadioptric optical system. Two wavebands share a non-confocal optical system that is used as the front-end telescope. A beamsplitter is used to split the emergent light into visible light and LWIR. The refractive optical system employs a secondary telescope, a polarizer, and an objective to focus visible light and LWIR on the detector. The common-aperture multispectral and polarization optical imaging system is thus realized.

To reduce the system aberration, the conic surfaces, rather than aspheric surfaces, are employed in three mirrors, which can facilitate processing and alignment and reduce the manufacturing cost. The values of the parameters of the conic surfaces are shown in Table 1. We use spheric surfaces to describe all other surfaces of the visible and LWIR transmission systems.

Figure 6 shows the spot diagrams and modulation transfer function (MTF) plots of the whole common-aperture multispectral and polarization optical imaging system at a full FOV of 4.5°. Figures 6(a) and 6(b) show the spot diagrams and MTF plots of the visible-spectrum optical system with the common-aperture off-axis reflection optical system. The maximum RMS radius of the spot diagram is 4.86 μm, which is less than the minimum pixel size (5 μm) of common visible-light detector. Figures 6(c) and 6(d) show the spot diagrams and MTF plots of the LWIR optical system with the common-aperture off-axis reflection optical system. The maximum RMS radius of the spot diagram is 12.28 μm, which is less than the minimum pixel size (15 μm or 25 μm) of common LWIR detector. The MTF plots of both wavebands are close to the diffraction limits as illustrated in Figs. 6(b) and 6(d). These characteristics satisfy the technical requirements.

Table 1. Values of parameters of off-axis reflection optical system.

Surfaces	*Y* radius	Conic constant
First mirror	−1,242.34	−0.96
Second mirror	−581.62	−4.98
Third mirror	1,022.17	−1.30

We have just finished the optical design of the system and set about mechanical design and optical elements fabrication recently. This experiment has a long project cycle, high cost and considerable difficulty. The experimental results will be shown in detail when the fabrication and alignment of the system are completed in the near future.

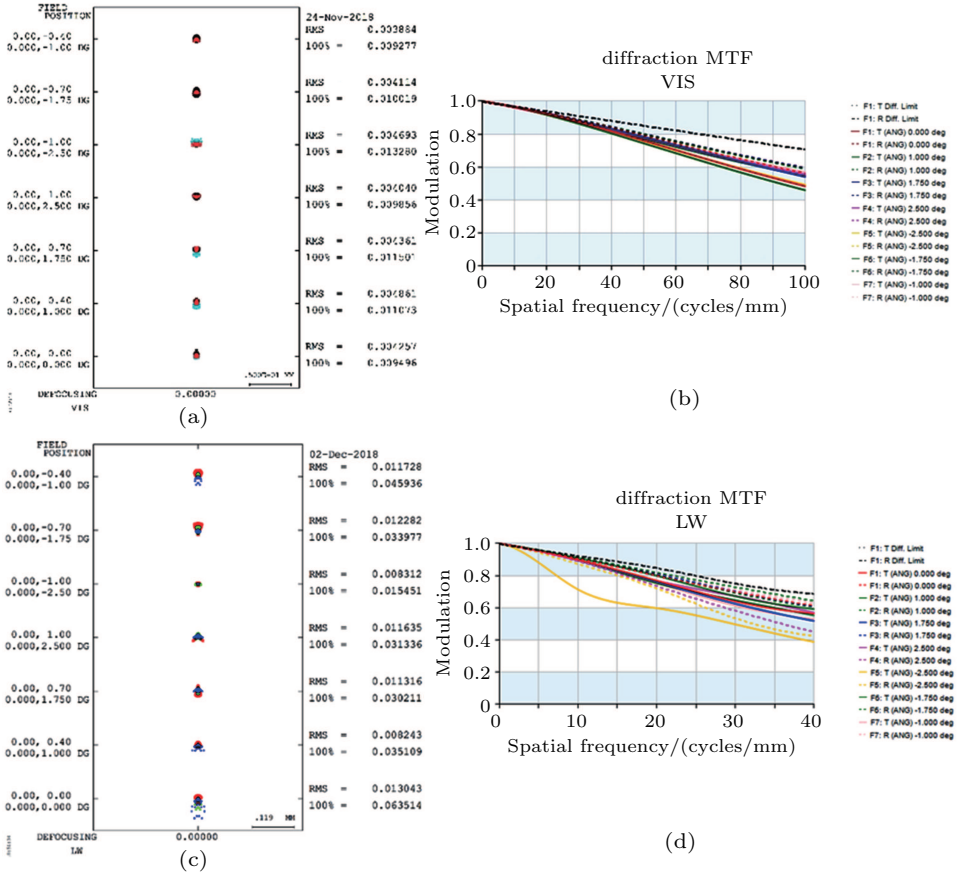


Fig. 6. Spot diagram and MTF plots of the common-aperture multispectral and polarization optical imaging system. (a) Spot diagram of visible-spectrum optical system and (b) its corresponding MTF plot. (c) Spot diagram of the LWIR optical system and (d) its MTF plot.

4. Conclusions

In this work, we introduce a common-aperture multispectral and polarization optical imaging system with a full FOV of 4.5°. Instead of incorporating two discrete transmission systems, we employ an off-axis three-mirror optical system as a front-end common-aperture telescope to improve the target discrimination and identification rates and reduce the false alarm rate. This system can maintain a wide FOV and enhance the identification ability of the system. At the same time, the off-axis three-mirror system gets rid of central obscuration but maintains the resolution and energy of the whole system. The whole system is composed of the reflective and refractive component. The reflective component employs an off-axis three-mirror optical system. The refractive component is divided into visible light and LWIR wavebands by a beamsplitter and they are converged on two detectors through two groups of lenses. This system enables the simultaneous acquisition of the spatial, spectral, and polarization information of a target. Given these characteristics, this system indicates remarkable potential applications in target detection and biomedical imaging.

References

[1] Sellar R G and Boreman G D 2005 *Opt. Eng.* **44** 013602
[2] Gowen A A, O'Donnell C P, Cullen P J, Downey G and Frias J M 2007 *Trends Food Sci. & Technol.* **18** 590
[3] Levenson R M and Mansfield J R 2006 *Cytometry, Part. A: Journal Int. Soc. For Anal. Cytology* **69** 748
[4] Chen J, Cai F, He R and He S 2018 *Sens.* (Basel Switzerland) **18** 1989
[5] Abdlaty R, Orepoulos J, Sinclair P, Berman R, Fang Q 2018 *Photonics* **5** 3
[6] Djokam M, Sandasi M, Chen W, Viljoen A, Vermaak I 2017 *Appl. Sci.* **7** 268 (in Chinese)
[7] Cai Q S, Huang M, Han W, Liu Y X and Lu X N 2018 *Acta Phys. Sin.* **67** 234205 (in Chinese)
[8] Tyo J S, Goldstein D L, Chenault D B and Shaw J A 2006 *Appl. Opt.* **45** 5453
[9] Jacques S L, Ramella-Roman J C, Lee K 2002 *J. Biomed. Opt.* **7** 329
[10] Ushenko V, Sdobnov A, Syvokorovskaya A, Dubolazov A, Vanchulyak O, Ushenko A, Ushenko Y, Gorsky M, Sidor M, Bykov A and Meglinski I 2018 *Photonics* **5** 54
[11] van Harten G, Snik F, Rietjens J H H, Martijn Smit J, Keller C U 2014 *Appl. Opt.* **53** 4187
[12] Tsai T H and J Brady D 2013 *Appl. Opt.* **52** 2153
[13] Shkuratov Y, Opanasenko N, Zubko E, Grynko Y, Korokhin V, Pieters C, Videen G, Mall U and Opanasenko A 2007 *Icarus* **187** 406
[14] Pierangelo A, Manhas S, Benali A, Fallet C, Totobenazara J L, Antonelli M R, Novikova T, Gayet B, De Martino A and Validire P 2013 *J. Biomed. Opt.* **18** 046014
[15] Garcia M, Davis T, Marinov R, Blair S and Gruev V 2018 *SPIE Commercial + Sci. Sens. Imaging*, April 16–17, 2018, Orlando, USA 10655C
[16] Mathews S A 2008 *Appl. Opt.* **47** F71
[17] Yu M, Liu T, Huang H, Hu H and Huang B 2016 *IEEE Photon. J.* **8** 1
[18] Gao L, Kester R T and Tkaczyk T S 2009 *Opt. Express* **17** 12293
[19] Snik F, Rietjens J, Harten G, Stam D, Keller C, Smit M, Laan E, Verlaan A, van der Horst R, Navarro R, Wielinga K, G Moon S and Voors R 2010 *SPIE Astronomical Telescopes Instrumentation*, June 22–July 2, 2010, San Diego, USA, 77311B
[20] Pacheco S and Liang R 2014 *Opt. Express* **22** 16377
[21] Manakov A, Restrepo J, Klehm O, Hegedüs R, Eisemann E, Seidel H P and Ihrke I 2013 *ACM Trans. Graph.* **32** 47
[22] Shinoda K, Ohtera Y and Hasegawa M 2018 *Opt. Express* **26** 15948
[23] Alouini M, Goudail F, Réfrégier P, Lallier E and Grisard A 2004 *SPIE Defense Security Symposium Remote Sensing VI*, July 15–17, 2004, Orlando, USA, p. 133
[24] Gupta N 2005 *J. Biomed. Opt.* **10** 051802
[25] Knitter S, Hellwig T, Kues M and Fallnich C 2011 *Opt. Lett.* **36** 3048
[26] Thompson N A 2013 *Opt. Eng.* **52** 061308
[27] Mahmoud A, Xu D and Xu L 2016 *SPIE Asia-Pacific Remote Sensing*, April 30, 2016, New Delhi, India, p. 6
[28] Song D L, Chang J, Zhao Y F and Zhang Z X 2018 *Chin. Phys. B* **27** 094220